Density-Diffusive Model of the Ninetyeast Ridge Current

ERIC S. JOHNSON[1]

Department of Oceanography, University of Washington, Seattle 98195

BRUCE A. WARREN

Woods Hole Oceanographic Institution, Woods Hole, MA 02543

15 February 1979

ABSTRACT

A model for the structure of deep western boundary currents, based on linear momentum equations and lateral mixing of density, is applied to data from a recent section across the Ninetyeast Ridge current in the eastern basin of the Indian Ocean. It accounts moderately well for the breadth of the current, as inferred from the density distribution, and for the form of its velocity profile, as inferred (roughly) from the silica distribution.

Linear dynamics, coupled with a balance between vertical advection and lateral diffusion of density (exchange coefficient $\approx 10^7$ cm^2 s^{-1}), has rationalized somewhat successfully the observed structure of the deep western boundary current of the South Pacific. The specific model considered a continuously stratified ocean, and resolved fields of interest into interior fields (given by observation and treated as uniform over the breadth of the boundary current) and western-boundary correction fields that decay eastward to zero. Specification of the vertical variation in density at the western boundary and application of upper and lower boundary conditions then allowed the latter fields to be calculated. The reader is referred to Warren (1976) for assumptions, mathematical development, physical interpretation and sensitivity of results to parameter choices.

For analytical tractability the ocean bottom was taken as level and the western boundary as "vertical", in the sense that its lateral displacement over its range of depth was much less than the width of the current. Not all deep western boundary currents meet these geometric restrictions (e.g., the bottom water currents along South America and Madagascar), but one that seems to do so, about as well as that in the South Pacific, is the Ninetyeast Ridge current of the West Australian Basin in the eastern Indian Ocean (Warren, 1977; Fig. 1 here). It therefore invites examination in terms of the density-diffusive model, as a further assessment of the importance of the dynamical elements included there.

Let (x,z) be the eastward and vertical coördinates, and assume that in the deep western boundary current zonal derivatives are much larger than meridional derivatives, and meridional velocities are much larger than zonal velocities. The density balance for the western-boundary correction field is approximated as

$$-wE\rho_0 = K\rho_{xx}, \tag{1}$$

where ρ and w are the correction fields for the density and vertical velocity, K the (constant) lateral diffusivity, ρ_0 a mean density (1.0 g cm^{-3}), and E the static stability associated with the full density field, which is due mainly to the interior field, and is to be taken from observations; it is convenient to represent E as $Bb(z)$, where $b(z)$ is a form function, and the constant B sets the magnitude. Combining (1) with appropriate linear viscous momentum equations [see Warren (1976) for details] gives a single equation for the correction pressure p, i.e.,

$$p_{xxxx} + \frac{f^2K}{AgB}\left(\frac{1}{b}p_{xxxx} - \frac{b'}{b^2}p_{xxx}\right) - \frac{\beta}{A}p_x = 0, \tag{2}$$

which has separable solutions $p = F(z)G(x)$:

$$F'' - \frac{b'(z)}{b(z)}F' + k^3b(z)F = 0, \tag{3}$$

$$G'''' - \frac{Kf^2k^3}{AgB}G'' - \frac{\beta}{A}G' = 0, \tag{4}$$

where f is the Coriolis parameter, β its meridional derivative, A the horizontal viscosity, g the acceleration due to gravity, and k^3 a positive separation constant, for which discrete values are selected by upper and lower boundary conditions.

As a station representative of the western interior field, against which to calculate the western-boundary correction field of density, we have chosen *Atlantis* II Station 2317 (Fig. 1). It lies to the west of stations 2318–2324, where the minimum in specific volume anomaly is found at depths of 3700–4000 m, evidently a feature of the eastern interior field, but to

[1] Present affiliation: Scripps Institution of Oceanography, University of California, San Diego 92093.

0022-3670/79/061288-06$05.50

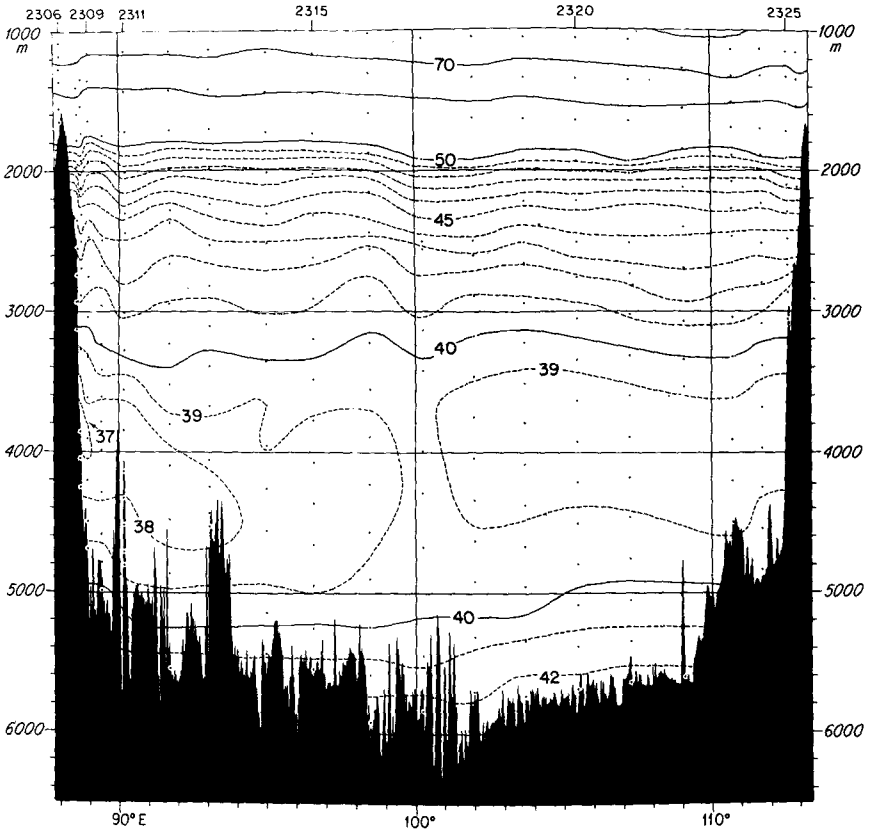

FIG. 1. Profile of specific volume anomaly (10^{-5} cm^3 g^{-1}) below 1000 m along latitude 18°S in the West Australian Basin of the Indian Ocean. Ninetyeast Ridge is on left, Australia on right. *Atlantis* II stations 2306–2326, 7–17 August 1976; station numbers on top, locations of observations indicated by dots. The deep western boundary current of the eastern Indian Ocean is marked roughly by sloping isanosteres below about 3000 m between Ninetyeast Ridge and Station 2314.

the east of stations 2312–2316, where the substantially greater depth of the minimum (4200–4500 m) seems to be associated with the western boundary field. Station 2317 may "look" somewhat anomalous, in that the minimum there is slightly greater (by 0.5×10^{-5} cm^3 g^{-1}) than at the adjacent stations, but the temperature-salinity relation for Station 2317 is entirely consistent with those for neighboring stations.

To avoid dealing with the thermocline, which is not of interest here anyway, it is convenient to adopt some observational feature at mid-depth as an upper boundary condition, rather than a more general condition at the sea surface: following Warren (1976), we observe that at *Atlantis* II stations 2307–2317 the vertical derivative of observed density correction is generally zero near 2200 m, suggesting for an upper boundary condition that one take $\rho_z = p_{zz} = 0$ at that level. For the bottom boundary condition, we treat the ocean bottom as level at 5000 m, whereby it is required that $w = 0$ there—or by (1), $\rho = 0$.

Boundary conditions in x are that p and p_x (i.e., G and G') $\to 0$ as $x \to \infty$, and that at the western boundary the meridional velocity $v = 0$ (no slip), and $\rho_x = 0$ (no mass flux through the boundary). Since the last two are redundant through the hydrostatic relation, however, both requiring simply that $G'(0) = 0$, a fourth condition is needed, which we meet by specifying ρ from observation at the western boundary.

Plots of E vs z in the western part of the basin (Fig. 2) suggest a linear representation of $E(z)$ below 2000 m: $b(z) = z$ and $B = 3.55 \times 10^{-15}$ cm^{-2}, with z set to zero at a depth of 5300 m. For eigenvalues k_n, solutions of (3) are then

$$F_n = C_n[\mathrm{Ai}'(-k_n z) + D_n \mathrm{Bi}'(-k_n z)], \qquad (5)$$

where Ai′ and Bi′ are the derivatives of the Airy functions, k_n and D_n are determined by the boundary conditions above on F and the C_n are arbitrary. Values of k_n and D_n for the three lowest order eigenfunctions are listed in Table 1, and the vertical derivatives of these functions (i.e., the density eigen-

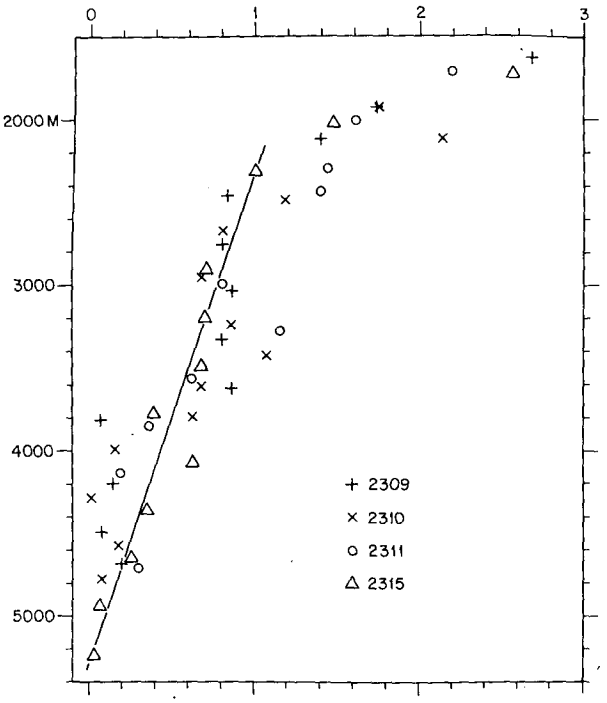

FIG. 2. Plots of static stability E (10^{-9} cm^{-1}) against depth for indicated *Atlantis* II stations on latitude 18°S in the western part of the West Australian Basin. Straight line indicates linear representation used in theoretical calculations.

functions) are plotted in Fig. 3. The constants C_n are to be chosen to match $\rho(0,z)$ to observation. Values of the measured correction density at the western boundary are plotted at 100 m intervals in Fig. 4, as constructed from smooth curves of specific volume anomaly for *Atlantis* II stations 2307–2309 less values at the same levels at station 2317. Least-squares fits to these data were calculated for combinations of both the first two density eigenfunctions and the first three (Fig. 4). The three-function fit is certainly not perfect, especially in its underestimate of the maximum at 3800 m, but it is so much better than the two-function fit that we have used it in our modeling of the Ninetyeast Ridge current,[2] despite the small vertical scale of the third eigenfunction, which makes questionable the neglect of vertical mixing in (1), and, as remarked below, its very large horizontal scale, which makes the separation between interior and boundary fields somewhat unclear. The relative contributions of the three eigenfunctions graphed in Fig. 3 to the density field at $x = 0$ are then $(C_2k_2)/(C_1k_1) = 1.08$ and $(C_3k_3)/(C_1k_1) = 0.86$—roughly equal.

With the eigenvalues k_n specified, the bounded solutions of (4) may be obtained in the form

$$G_n(x) = \mathrm{Re}[P_n(e^{-\alpha_{1n}x} + Q_n e^{-\alpha_{2n}x})],$$

[2] This contrasts with the deep western boundary current of the South Pacific, where Warren (1976) found that only the first two eigenfunctions were needed for as good a fit.

TABLE 1. Eigenfunction parameters.

Mode no. n	k_n (km^{-1})	D_n	α_{1n} (10^{-2} km^{-1})	α_{2n} (10^{-2} km^{-1})
1	0.614	−0.0757	2.20 + 0.330i	2.20 − 0.330i
2	1.206	−0.994	10.4	0.198
3	1.697	−0.127	17.4	0.0714

where the constants, P_n, Q_n are determined by the boundary conditions $G(0) = 1$, $G'(0) = 0$ (see Warren, 1976). The parameters we have used in the calculations are $f = 0.45 \times 10^{-4}$ s^{-1}, $\beta = 2.2 \times 10^{-13}$ cm^{-1} s^{-1}, $g = 980$ cm s^{-2}, $K = A = 1.0 \times 10^{7}$ cm^2 s^{-1} (a conventional estimate). The resulting values of α_{1n}, α_{2n} are listed in Table 1 for $n = 1$, 2 and 3. The first-order horizontal eigenfunction has a small width, about 50 km, while the second and third are quite broad, with e-folding scales of 505 and 1400 km. Given that our "interior" station, station 2317, is only ~1200 km from the western boundary, it does not really seem to be out of the boundary field if the third eigenfunction is an important part of it. In trying to adapt this boundary-layer approach to the interpretation of oceanographic data, however, there must evidently be some compromise in identifying a station that is both representative of the western interior field and free of western-boundary phenomena.

For ease of comparison with Fig. 1, the calculated field of western-boundary correction density has been converted to specific volume and added to the specific volume anomaly at station 2317 to produce

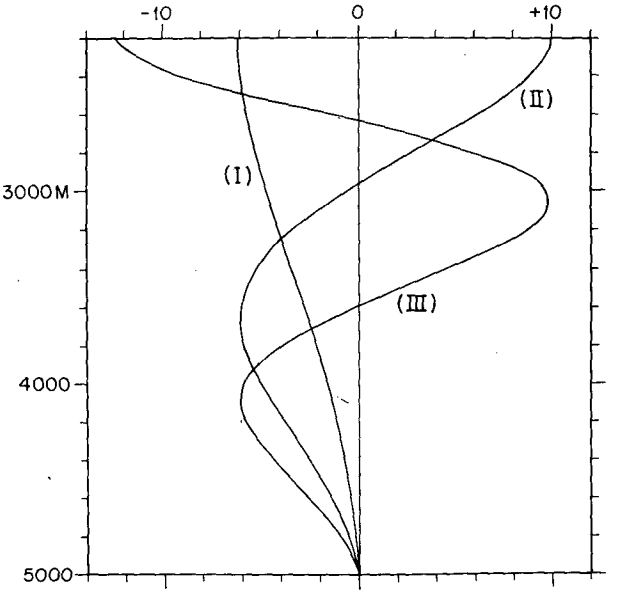

FIG. 3. Variation with depth of the three lowest order eigenfunctions for correction density, equivalent to vertical derivatives of eigenfunctions for correction pressure. Amplitudes are arbitrary.

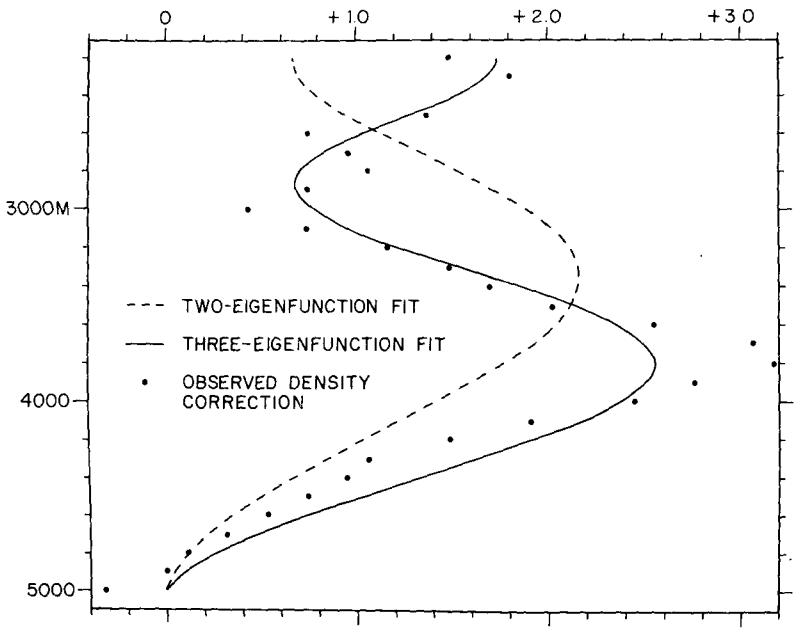

FIG. 4. Dots: "observed" values of correction density (10^{-5} g cm^{-3}) at Ninetyeast Ridge, constructed from observations at *Atlantis* II stations 2307–2309 with reference to station 2317. Dashed line: least-squares fit of a combination of the first two density eigenfunctions (Fig. 3) to observed correction densities. Solid line: least-squares fit of a combination of the first three eigenfunctions.

a theoretical field of total specific volume anomaly for the boundary current (Fig. 5). Since the theoretical field has been fitted (roughly) to observation at its western and eastern ends, it is only its pattern in between, of course, that can be tested against Fig. 1. The minimum near 4000 m descends to the eastward, about as much as observed, and about at the right rate, if the noisiness of the observed field is discounted, although the 38-isanostere does not reach far enough to the east, and the 39-isanostere extends too far—the latter because the very large horizontal scale of the third eigenfunction prevents the theoretical correction field from decaying to something insignificant at station 2317. Also the calculated isanosteres of 41–43 × 10^{-5} cm^3 g^{-1} are generally 100–200 m too deep. Overall, for a conven-

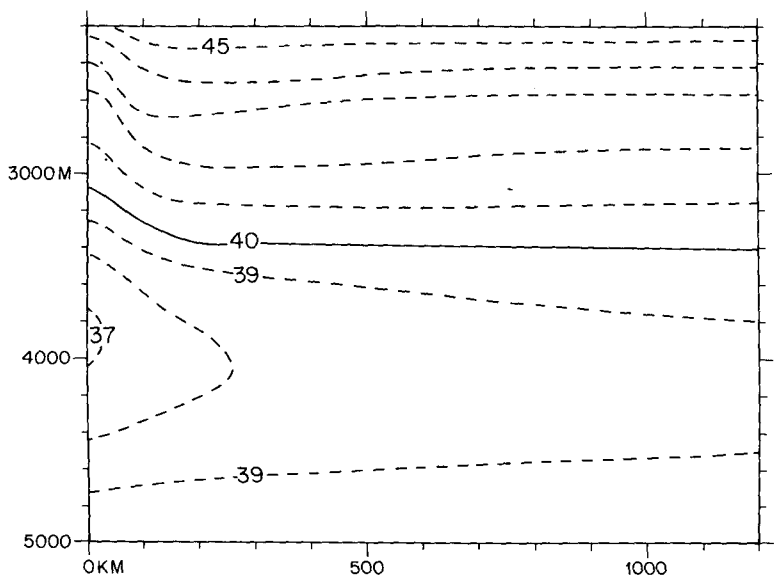

FIG. 5. Theoretical field of total specific volume anomaly (10^{-5} cm^3 g^{-1}) for Ninetyeast Ridge current; cf. Fig. 1.

tional value of the horizontal diffusivity, the calculated field looks good in comparison with observation but not excellent.

In the corresponding field of calculated meridional velocity (Fig. 6), the flow is weak, ~0.1 cm s^{-1}, in the eastern part of the boundary current, and is southward above about 4000 m and northward below. The relatively swift flow is confined to within about 200 km of the western boundary, and the maximum northward velocity, nearly 4 cm s^{-1}, is found at the bottom, 70 km from the boundary. Moreover, the lower zero-isotach rises toward the boundary, such that much of the weak southward flow is separated from the boundary by relatively intense northward flow.

There are no velocity measurements to compare with Fig. 6, but the distribution of dissolved-silica concentration along 18°S in the West Australian Basin (Fig. 7) offers some hints about the pattern of deep flow. As in the southwestern Pacific, there is a deep silica maximum, here centered at ~3000 m; it indicates southward flow from the high-silica region to the north, lying about northward flowing, relatively low-silica water from the Antarctic (Wyrtki, 1971). The depth of reversal in flow direction is not defined precisely by these data, but the calculated depth of 4000 m (Fig. 6) is at least consistent with the observed pattern of silica variation. Also as in the southwestern Pacific, the silica maximum does not extend all the way to the western boundary of the basin, but is separated from it by a 200 km wide zone of relatively low-silica water, suggestive of northward flow within that zone, much as shown in the calculated velocity profile (Fig. 6). In comparison with the silica profile (Fig. 7), however, the calculated zone of swift northward flow does not seem to reach quite shallow enough. By contrast, the calculation for the South Pacific (Warren, 1976) gave northward flow close to the boundary all the way from the bottom to 2000 m, and thereby made a better match to the silica distribution. On the other hand, in the eastern part of that current the silica distribution showed that the calculated depth of reversal in flow direction was at least 300 m too deep, whereas it looks roughly right in our present calculation for the Ninetyeast Ridge current. Although the deep silica differences in the West Australian Basin are smaller, and therefore of less certain pattern, than those in the southwestern Pacific, they still provide good support for the form of the calculated deep western boundary current there.

An unsatisfying aspect of this calculation is its reliance on an empirical upper boundary condition at mid-depths, because the larger-scale trends in the density data here are small enough to be obscured somewhat by the small-scale fluctuations, and observational features stand out less clearly in the West Australian Basin than in the southwestern Pacific. For example, from inspection of the *Atlantis* II station data one might persuade himself almost as well that $\rho = 0$ near 2000 m as that $\rho_z = 0$; and the former condition could not have led to northward flow between the western boundary and the weak southward flow offshore. Our justification for our particular choice of upper boundary condition is therefore somewhat *ad hoc*: that it is a condition consistent with the density data (with due allowance for noise) that does produce a velocity profile rationalizing—qualitatively—the silica distribution.

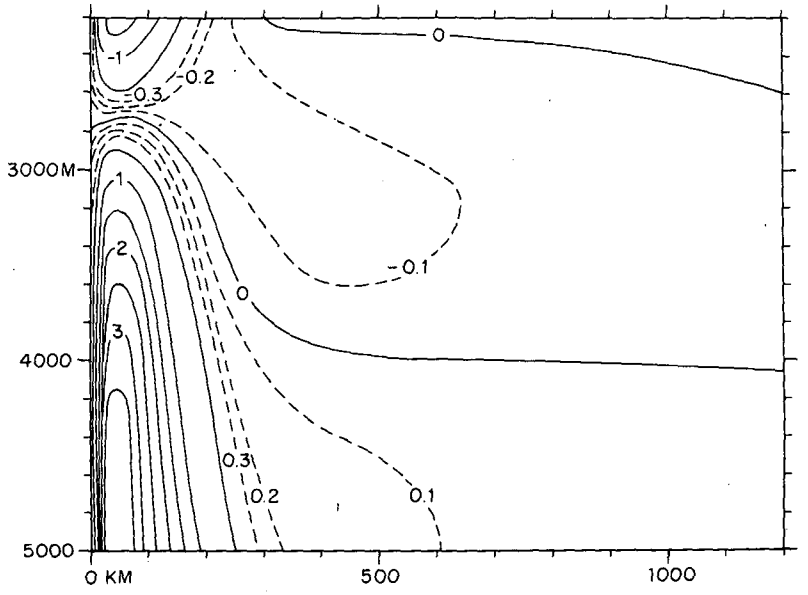

FIG. 6. Theoretical profile of meridional component of velocity (cm s^{-1}) for Ninetyeast Ridge current. Positive velocities are northward, negative southward. Solid isotachs are at intervals of 0.5 cm s^{-1}; dashed isotachs, 0.1 cm s^{-1}.

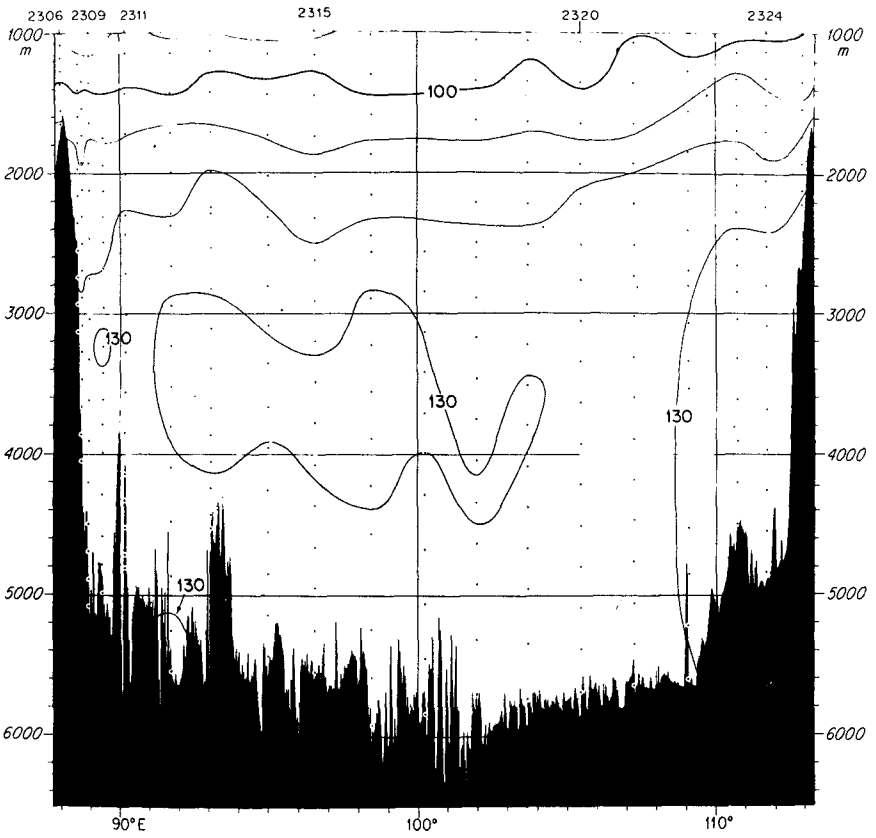

FIG. 7. Profile of dissolved-silica concentration (μg-atm ℓ^{-1}) below 1000 m along latitude 18°S in the West Australian Basin. See caption to Fig. 1.

Another, but lesser, cause for dissatisfaction is the somewhat uncertain basis for choosing a reference station for calculating correction densities. This uncertainty is more troublesome in the present calculation than in that for the southwestern Pacific, partly because the theoretical correction field turns out to be broader here, and partly because overall property contrasts are smaller here, whereby uncertainty in the resulting values of measured correction density at the western boundary is of more concern in determining the eigenfunction fit. Details of our calculation are thus questionable for this reason, but the general features are probably not.

Finally, we are as uneasy as was Warren (1976) about the concept of lateral mixing of density, which is the crucial dynamical element in this current model, and dissatisfied as well with the eddy-coefficient parameterization, especially close to the western boundary. Nevertheless, for the deep western boundary currents of both the South Pacific and the West Australian Basin, that concept accounts at once for two features that must be considered essential to any successful rationalization of the current structure. First, for diffusivity values familiar from other and quite different investigations, it gives flow fields having the great breadth characteristic of deep western boundary currents, something no other level-bottom model has been able to explain. Second, it produces eigenfunctions whose horizontal scale varies inversely with their vertical scale, a necessary property for the construction of a velocity profile in which a vertically extensive zone of northward flow close to the western boundary abuts a region to the east of southward flow above and northward flow below. That the model has worked as well as it has for two different currents suggests that there must be some truth in it.

Acknowledgments. This work was done while E.J. was a recipient of a Summer Student Fellowship at the Woods Hole Oceanographic Institution, for which he is grateful. Support for B.W. was provided by the Office of Naval Research under Contract N00014-74-C-0262, NR 083-004.

REFERENCES

Warren, Bruce A., 1976: Structure of deep western boundary currents. *Deep-Sea Res.*, **23**, 129–142.

——, 1977: Deep western boundary current in the eastern Indian Ocean. *Science*, **196**, 53–54.

Wyrtki, K. (1971): *Oceanographic Atlas of the International Indian Ocean Expedition.* National Science Foundation, Washington, DC, 531 pp. + xii pp.